A Case Study of Focal Bayesian EEG Inversion for Whitney Element Source Spaces: Mesh-Based vs. Cartesian Orientations

T. Miinalainen[1] and S. Pursiainen[1]

[1] Tampere University of Technology, Department of Mathematics, PO Box 692, 33101 Tampere, Finland. Email: sampsa.pursiainen@tut.fi.

Abstract— **This paper concentrates on the Bayesian detection of the neuronal current distributions in the electroencephalography (EEG) imaging of the brain activity. In particular, we focus on a hierarchical *maximum a posteriori* inversion technique applicable when the lead field matrix is constructed via the finite element method. We utilize the linear Whitney (Raviart-Thomas) basis functions as source currents. In the numerical experiments, the accuracy was investigated using two spherical head models. The results obtained suggest that the interpolation of the dipolar source space does not necessarily bring any advantage for FEM based inverse computations. Furthermore, the divergence conforming Whitney-type sources were found to be sufficient for precise and highly focal Bayesian modeling of dipole-like currents.**

Keywords— **Hierarchical Bayesian inverse model, Electroencephalography (EEG), Finite Element Method (FEM), Whitney elements**

I. Introduction

The aim of this study is to compare two types of finite element method (FEM) sources for hierarchical Bayesian [1] Electroencephalography (EEG) imaging. In reconstructing the neural activity in the brain, it is crucial that the source of the impulse can be approximated as focally as possible [2, 3]. In this study, we show that source reconstruction is feasible directly using the Whitney (Raviart-Thomas) type source functions which for an unstructured tetrahedral finite element mesh have random orientations. The direct approach is compared to a classical approach in which the sources are interpolated into a regular Cartesian grid before the inversion of the measurements.

Finite element method is a versatile simulation method for discovering numerical solutions of boundary value problems for partial differential equations [4]. In particular, the FEM enables creating a volumetric tetrahedral mesh that is an accurate model of the head geometry regarding its internal folded surfaces [5] and also the conductivity structure. Additionally, the FEM makes it possible to incorporate detailed 3D structures (skull compacta, spongiosa) and the anisotropic conductivity of the white matter into the EEG forward simulation. [6, 5]. An extensive overview of EEG forward modeling with FEM is presented in [3].

In this study, we harness the divergence conforming H(div) vector basis functions which provide a mathematically rigorous approach to source modeling [2, 7]. Of the several available options for H(div) finite element basis functions, we use the linear Whitney (Raviart-Thomas) basis functions which can be interpreted as dipolar sources with a face intersecting orientation in the finite element (FE) mesh [8]. Continuing the recent forward simulation study [2], we here compare the inversion accuracy obtained (i) directly with the FE mesh based Whitney sources and (ii) with interpolated Cartesian source orientations. The case (i) is the most straightforward approach when vector basis functions with random positions and orientations corresponding to an unstructured FE mesh can be used. As regular point lattices are, however, necessary for the function of numerous inversion methods [9], the case (ii) is generally used in EEG imaging.

The hierarchical Bayesian approach [10, 11] explored in this paper allows using both (i) and (ii) type sources and thus investigating the inverse aspect of the difference between them. The primary source current density is associated with a conditionally Gaussian prior the variance of which is assumed to be distributed according to a gamma or inverse gamma hyperprior. We use the iterative alternating sequential (IAS) *maximum a posteriori* estimation algorithm [10] to find a large set of reconstructions which is analyzed in terms of box-plots for different eccentricity (relative norm) values. The distance, orientation and magnitude differences between the reconstructed sources and analytic dipoles are measured.

II. Materials and Methods

A. Forward Model

The EEG forward problem is to find the electric potential field u on the surface $\partial\Omega$ of the domain (head model) Ω given a pointwise symmetric and positive definite conductivity tensor distribution σ and the primary current density $\vec{J}^{\mathcal{P}}$ in Ω. The potential field u can be predicted by solving the Poisson type equation $\nabla\cdot(\sigma\nabla u) = \nabla\cdot\vec{J}^{\mathcal{P}}$ in Ω with the homogeneous Neumann the boundary condition $(\sigma\nabla u)\cdot\vec{n} = 0$

H. Eskola et al. (eds.), *EMBEC & NBC 2017*,
IFMBE Proceedings 65,
DOI: 10.1007/978-981-10-5122-7_266

given on Ω. Multiplying both sides of this equation with the test function v and integrating it by parts over Ω results in the the weak form $\int_\Omega \nabla v \cdot (\sigma \nabla u)\, dV = -\int_\Omega v(\nabla \cdot \vec{J}^P)\, dV$, for all $v \in H^1(\Omega)$. Here $H^1(\Omega)$ is the Sobolev space consisting of functions with all first-order partial derivatives square integrable, i.e., in $L_2(\Omega)$. The solution $u \in H^1(\Omega)$ for the weak form is unique up to choosing the zero level of the potential, if the divergence of the primary current density is a square integrable. In other words, if$J^P \in H(\mathrm{div}) = \{\vec{w} \,|\, \nabla \cdot \vec{w} \in L^2(\Omega)\}$ [2, 12, 4].

We assume that the domain Ω has been subdivided into a set of unstructured tetrahedral finite elements and that u belongs to a subspace $S \subset H^1(\Omega])$ spanned by finite-element basis functions. The potential distribution is approximated via $u_h = \sum_{i=1}^N z_i \psi_i$ with piecewise linear nodal basis functions $\psi_1, \psi_2, \ldots, \psi_N$. Similarly, the primary current distribution can be estimated via $\vec{J}_h^P = \sum_{j=1}^K x_j \vec{w}_j$ with basis functions $\vec{w}_1, \vec{w}_2, \ldots, \vec{w}_K \in H(\mathrm{div})$. The corresponding coordinate vectors $\mathbf{z} = (z_1, z_2, ..., z_N)$ and $\mathbf{x} = (x_1, x_2, ..., x_K)$ refer to the solution of the linear system $\mathbf{Az} = \mathbf{Gx}$ where $\mathbf{A} \in \mathbb{R}^{(N \times N)}$, $\mathbf{G} \in \mathbb{R}^{(N \times K)}$, $A_{i,j} = \int_\Omega \nabla \psi_j \cdot (\sigma \nabla \psi_i)\, dV$ and $G_{i,j} = \int_\Omega \psi_i (\nabla \cdot \vec{w}_j) dV$. An electrode voltage vector $\mathbf{y}$ can be composed as $\mathbf{y} = \mathbf{RA}^{-1}\mathbf{Gx} = \mathbf{Lx}$, where $\mathbf{R}$ defines a restriction matrix by picking the potential (voltage) values at the electrode locations and defining the zero potential level, e.g., as the mean of the measurements $\mathbf{y}$. If the ℓ-th electrode on $\partial\Omega$ is located at the i_ℓ-th node, then $R_{\ell,i_\ell} = 1 - 1/L$, and also if $\ell \neq j$, then $R_{\ell,i_j} = -1/L$ and finally, $R_{\ell,j} = 0$ if there exists no electrode associated with the j-th node. [2]

B. Mesh-based Dipolar Sources

The primary source current of the neuronal activity is modeled in this study with synthetic dipolar sources. For this purpose, we utilize divergence conforming Whitney (Raviart-Thomas) function basis. The dipole moment and the position of a synthetic dipole can be defined as follows [8, 2]:

$$\vec{q}_{\vec{w}} = \frac{\vec{r}_{P_j} - \vec{r}_{P_i}}{\|\vec{r}_{P_j} - \vec{r}_{P_i}\|} \quad \text{and} \quad \vec{r}_{\vec{w}} = \frac{1}{2}(\vec{r}_{P_i} + \vec{r}_{P_j}), \tag{1}$$

where $\vec{r}_{P_i}$ and $\vec{r}_{P_j}$ are the position vectors of mesh nodes P_i and P_j on the opposite sides of the face determining the Whitney basis function. The synthetic dipole moment follows from the definition $\vec{q}_{\vec{w}} = \int_\Omega \vec{w}\, dV$. The position is defined as the midpoint of the nodes P_i and P_j. A straightforward calculation [8] shows that the entries of the matrix $\mathbf{G}$ are of the form $G_{\psi,\vec{w}} = \int_\Omega \psi(\nabla \cdot \vec{w}) dV = (s_{\{\psi,P_j\}} - s_{\{\psi,P_i\}})/\|\vec{r}_{P_j} - \vec{r}_{P_i}\|$ for a given pair ψ, $\vec{w}$ of basis functions with $s_{\{\psi,P\}} = 1$, if ψ corresponds to node P and $s_{\{\psi,P\}} = 0$, otherwise. The synthetic dipoles are resolved more extensively, e.g., in [8, 2].

C. Interpolation to Cartesian Orientations

In this study, we compare the mesh-based orientations following from Equation (1) to interpolated Cartesian orientations. We use the position-based optimization [8] which approximates a given dipole with position $\vec{r}$ and dipole moment $\vec{p}$ as a superposition of the synthetic dipolar sources, i.e., $\vec{r} \approx \sum_{\ell=1}^M c_\ell \vec{r}_{\vec{w}_\ell}$ and $\vec{p} \approx \sum_{\ell=1}^M c_\ell \vec{q}_{\vec{w}_\ell}$. The coefficient vector $\mathbf{c} = (c_1, c_2, \ldots, c_M)$ is found as the solution of the linear system $\min_{\mathbf{c}} \sum_{\ell=1}^M c_\ell^2 \omega_\ell^2$ subject to $\mathbf{Qc} = \mathbf{p}$, where the parameter $\omega_\ell = \|\vec{r}_{\vec{w}_\ell} - \vec{r}\|_2$ is a weighting coefficient and the columns of $\mathbf{Q}$ are formed by the coordinate vectors $\mathbf{q}_{\vec{\mathbf{w}}_1}, \mathbf{q}_{\vec{\mathbf{w}}_2}, \ldots, \mathbf{q}_{\vec{\mathbf{w}}_M}$ of the synthetic dipole moments, i.e., $\mathbf{Q} = (\mathbf{q}_{\vec{\mathbf{w}}_1}, \mathbf{q}_{\vec{\mathbf{w}}_2}, \ldots, \mathbf{q}_{\vec{\mathbf{w}}_M})$. The constraint $\mathbf{Qc} = \mathbf{p}$ guarantees that the orientations of the interpolated and actual dipole will coincide. For the convexity of $\sum_{\ell=1}^M c_\ell^2 \omega_\ell^2$, the minimizer can be found utilizing the method of Lagrangian multipliers. In this study, four synthetical sources were utilized for each individual dipole approximation, matching with those Whitney basis functions associated with the tetrahedron (element) which contains the given dipole position.

D. Hierarchical Bayesian Inversion

The hierarchical Bayesian approach [10, 11, 1] refers here to formulating $\mathbf{x}$ as a random variable with the posterior density of the form $\pi(\mathbf{x}, \boldsymbol{\theta} \mid \mathbf{y})_{\mathrm{post}} \propto \pi_{\mathrm{hyper}}(\boldsymbol{\theta}) \pi_{\mathrm{pr}}(\mathbf{x} \mid \theta) \pi_{\mathrm{lh}}(\mathbf{x} \mid \mathbf{y})$ in which $\pi_{\mathrm{lh}}(\mathbf{x} \mid \mathbf{y})$ is a Gaussian likelihood of the measurements, $\pi_{\mathrm{pr}}(\mathbf{x} \mid \theta)$ is a conditionally Gaussian prior density, and $\pi_{\mathrm{hyper}}(\boldsymbol{\theta})$ is the prior of the hyperparameter $\boldsymbol{\theta} = (\theta_1, \theta_2, \ldots, \theta_K)$ the i-th entry of which determines the prior variance of x_i. Here, the Gamma distribution is determined by the shape and scaling parameter β and θ_0 (initial variance) is used as the hyperprior. The likelihood follows from the zero-mean Gaussian white noise model with standard deviation ν. The hierarchical Bayesian formulation is suitable for this study, in particular, as it allows finding a focal estimate for $\mathbf{x}$ independently of the vector basis of the primary current distribution. The realization, we apply the following iterative alternating sequential (IAS) algorithm [10]: Hence, the IAS algorithm can be written as:

1. Set $k = 0$ and $\boldsymbol{\theta}^{(0)} = (\theta_0, \theta_0, \ldots, \theta_0)$.
2. Set $\mathbf{L}^{(k)} = \mathbf{L}\mathbf{D}_{\theta^{(k)}}^{1/2}$ with $\mathbf{D}_{\theta^{(k)}} = \mathrm{diag}(|\theta_1^{(k)}|, |\theta_2^{(k)}|, \ldots, |\theta_n^{(k)}|)$.
3. Find $\mathbf{x}^{(k+1)} = \mathbf{D}_{\theta^{(k)}}^{1/2} \mathbf{L}^{(k)^T} (\mathbf{L}^{(k)} \mathbf{L}^{(k)^T} + \sigma^2 \mathbf{I})^{-1} y$.
4. Set $\theta_i = \frac{1}{2}\theta_0 \Big(\eta + \sqrt{\eta^2 + 2x_i^{(k)^2}/\theta_0}\Big)$ with $\eta = \beta - 3/2$, $i = 1, 2, \ldots, K$.

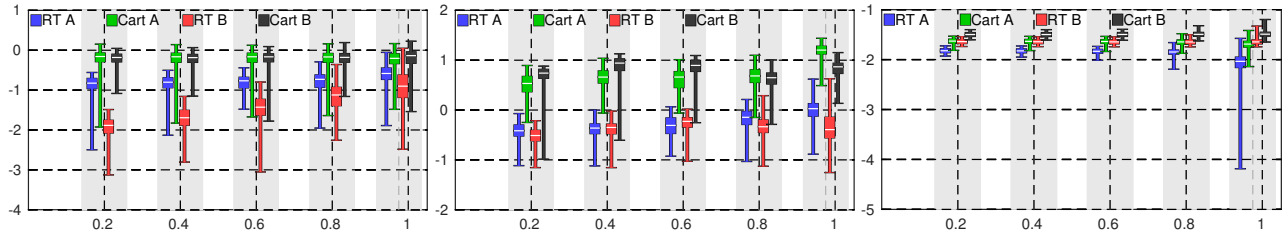

Fig. 1: The orientation (degrees), position (mm) and relative magnitude (unit less) error (left, center and right, respectively) on the common logarithmic scale (base 10) for both Whitney (Raviart-Thomas, RT) and Cartesian orientations. The case A corresponds to the Stok head model and case to the Ary model. The box-plot bars show the median, the interval between the maximum and minimum and the interval between upper and lower quartile.

5. Set $k = k + 1$ and go back to 2., if k is less than the total number of iterations defined by the user.

When $\beta = 3/2$, the applied inversion strategy can be interpreted as a special case of the classical minimum current estimate (MCE) [13] in which the ℓ^1-norm of the current density is used as a regularizing function in order to produce a focal reconstruction. Based on the *maximum a posteriori* estimate, the dipole location and direction of a single dipole is, in this study, estimated via the weighted averages $\vec{r} = \sum_{i=1}^{K} |x_i| \vec{r}_{w_i} / \sum_{i=1}^{K} |x_i|$, and $\vec{q} = \sum_{i=1}^{K} |x_i| \vec{q}_{w_i} / \sum_{i=1}^{K} |x_i|$.

E. Numerical Experiments

Two spherical multilayer models, the isotropic Ary [14] and anisotropic Stok model [15] were used in the numerical experiments. The first one consists of three layers, the brain, skull and scalp layer with radii 87, 92 and 100 mm and conductivities 0.33, 0.0042 and 0.33 S/m, respectively. The second one includes an additional cerebrospinal fluid (CSF) layer between the brain and the skull with the radii and conductivities being 78, 80, 86 and 92 mm and conductivities 0.33, 1.79, (0.042, 0.0042) and 0.33 S/m from the innermost to the outermost layer. In the Stok model the skull is anisotropic with the conductivity ratio 10:1 between the tangential and radial directions. The analytical dipole field for these models was estimated using the Zhang's method [16].

The dipole estimation accuracy was evaluated for five different eccentricity values, i.e., for five different relative radii w.r.t. the brain layer: 0.20, 0.40, 0.60, 0.80, and 0.99. For each of these values, 200 random analytic unit dipoles were generated. The analytic electric potential was evaluated at 200 equally distributed points on the outermost spherical surface. The amplitude of the potential was 3.1 and 1.6 μV for the Ary and Stok model, respectively. Gaussian white noise was added to the measurements with standard deviation $\nu = 0.2$, equaling to 6 and 13 % w.r.t. potential amplitude, respectively.

The number of nodes and tetrahedra in the finite element mesh generated for Ary and Stok consisted of 111161 and 113256 nodes and 617684 and 621952 tetrahedra, resulting in a total of 437981 and 440338 Whitney sources inside the brain layer, respectively. The interpolated Cartesian source orientations were generated for an equally spaced 2 mm three-dimensional grid of source positions leading to a total of 10070451 and 774462 sources, three for each grid point.

The shape and scaling parameter for the Gamma hyperprior were set to be $\beta = 1.5$ and $\theta_0 = 0.1$, respectively. The first choice is the smallest possible value and the second one is the initial guess for the prior variance. The number of IAS steps was chosen to be five. The inversion accuracy was measured evaluating the orientation (degrees), position (mm) and relative magnitude error between the reconstructed and analytic source.

III. Results

The results are presented in terms of box plots in Figure 1. For both Ary and Stok model, the inversion accuracy obtained with the mesh-based orientations was found to be superior compared to the Cartesian case. Regarding both orientation and position error, the difference between the mesh-based and interpolated estimates was close to one magnitude for all eccentricity values analyzed. For the relative magnitude the error was considerably smaller. At the eccentricity of 0.99, the median orientation error for the mesh-based approach was less than 0.3 degrees and for the Cartesian case it was over 0.6 degrees. The position error was less than 1 mm and larger than 6 mm for the mesh-based and Cartesian orientations, respectively. The largest magnitude error median was around 3 % in both cases.

IV. Discussion

In this paper, it was shown via numerical experiments that a hierarchical Bayesian inversion technique [10, 11] can be successfully applied to EEG inversion using Whitney type sources regardless of their orientation. In particular, we analyzed and compared the dipole detection accuracy obtained (i) directly with the mesh-based basis functions and (ii) with interpolated Cartesian source orientations. Formally, the most straightforward inversion estimate is obtained in the case (i), when interpolation is not used. The case (ii) is necessary for some inversion routines, e.g., sampling based approaches [9]. Sampling in the context of the present hierarchical Bayesian inversion is, however, possible in an unstructured mesh [10].

The outcome of the numerical experiments suggests that the divergence conforming Whitney-type sources are sufficient for precise and highly focal Bayesian modeling of dipole-like currents. Based on the results, it also seems that the interpolation of the dipolar source space does not necessarily bring any advantage for FEM based inverse computations. The significance of the differences between mesh-based and Cartesian orientation regarding clinical application is not obvious, since the magnitude of the errors depends strongly on the applied mesh resolution and geometry. A focal interpolation strategy uses a very local and limited set of basis functions to estimate a given source (here four), and therefore, the interpolation error does not tend to zero when the resolution goes up. Focality, on the other hand, is necessary for placing sources in the thin layers of the gray matter in order to avoid numerical errors [2, 3]. Since the Whitney basis functions utilize only two mesh nodes per a synthetic dipole source, they provide the most focal approach for modeling of dipolar sources. Consequently, analysis of the current direct mesh-based approach within a realistic geometry would be an important future study to further validate its significance in improving accuracy and focality of the inversion.

V. Conclusions

It was shown that a hierarchical Bayesian EEG inversion approach can be applied together with Whitney type dipole-like source currents with mesh-based directions. The non-interpolated dipolar sources outperformed the interpolated version in all three aspects explored, i.e., orientation, position and magnitude error. The present results strengthen the previous ones obtained for forward modeling [2]. Applying the non-interpolated inversion approach for a realistic geometry would be an important future work to validate its significance in improving accuracy and focality of the reconstructions.

Conflict of Interest

The authors declare that they have no conflict of interest.

Acknowledgements

TM and SP were supported by the Academy of Finland Key project (project 305055) and Academy of Finland Centre of Excellence in Inverse Problems Research.

References

1. O'Hagan Anthony, Forster Jonathan J. *Kendall's advanced theory of statistics, volume 2B: Bayesian inference*;2. Arnold 2004.
2. Pursiainen S, Vorwerk J, Wolters C H. Electroencephalography (EEG) forward modeling via H(div) finite element sources with focal interpolation *Physics in Medicine and Biology.* 2016;61:8502–8520.
3. Munck J.C., Wolters C. H., Clerc M.. EEG & MEG forward modeling. in *Handbook of Neural Activity Measurement* (Brette R., Destexhe A.. , eds.)Cambridge University Press, New York 2012.
4. Braess D. *Finite Elements*. Cambridge: Cambridge University Press 2001.
5. Vorwerk J, Cho J H, Rampp S, Hamer H, Knösche T R, Wolters C H. A guideline for head volume conductor modeling in EEG and MEG *NeuroImage.* 2014;100:590-607.
6. Hallez H., Vanrumste B., Van Hese P., Delputte S., Lemahieu I.. Dipole estimation errors due to differences in modeling anisotropic conductivities in realistic head models for EEG source analysis. *Phys.Med.Biol.*. 2008;53:1877–1894.
7. Ainsworth M, Coyle J. Hierarchic finite elements for unstructured tetrahedral meshes *Int. J. Numer. Meth. Engng.* 2003;58:2103–2130.
8. Bauer M, Pursiainen S, Vorwerk Johannes, Köstler Harald, Wolters C H. Comparison Study for Whitney (Raviart-Thomas) Type Source Models in Finite Element Method Based EEG Forward Modeling *IEEE Transactions on Biomedical Engineering.* 2015. Accepted for publication.
9. Calvetti Daniela, Somersalo Erkki. *An Introduction to Bayesian Scientific Computing: Ten Lectures on Subjective Computing*;2. Springer Science & Business Media 2007.
10. Calvetti D, Hakula H, Pursiainen S, Somersalo E. Conditionally Gaussian Hypermodels for Cerebral Source Localization *SIAM J. Imaging Sci.*. 2009;2:879–909.
11. Lucka Felix, Pursiainen Sampsa, Burger Martin, Wolters Carsten H.. Hierarchical Bayesian inference for the EEG inverse problem using realistic FE head models: Depth localization and source separation for focal primary currents *NeuroImage.* 2012;61:1364–1382.
12. Evans L.C.. *Partial Differential Equations*. Graduate studies in mathematicsAmerican Mathematical Society 1998.
13. Uutela K., Hämäläinen M., Somersalo E.. Visualization of Magnetoencephalographic Data Using Minimum Current Estimates *NeuroImage.* 1999;10:173–180.
14. Ary James P, Klein Stanley A, Fender Derek H. Location of sources of evoked scalp potentials: corrections for skull and scalp thicknesses *IEEE Transactions on Biomedical Engineering.* 1981:447–452.
15. Stok C J. The influence of model parameters on EEG/MEG single dipole source estimation *IEEE Trans. Biomed. Eng.*. 1987;34:289–296.
16. Zhang Z. A fast method to compute surface potentials generated by dipoles within multilayer anisotropic spheres *Phys. Med. Biol.*. 1995;40:335–349.